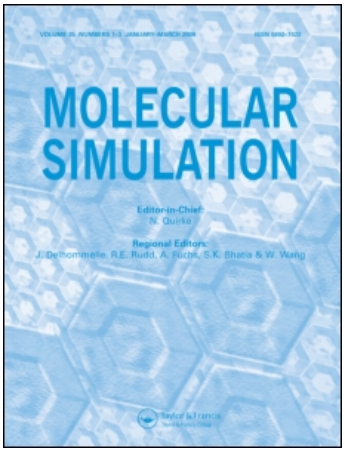

Molecular Simulation
Publication details, including instructions for authors and subscription information:
http://www.informaworld.com/smpp/title~content=t713644482

Motions of ions in a nanoscale Paul trap from molecular dynamics

Xiongce Zhao[a]
[a] Oak Ridge National Laboratory, Center for Nanophase Materials Sciences, Oak Ridge, TN, USA

To cite this Article Zhao, Xiongce(2009) 'Motions of ions in a nanoscale Paul trap from molecular dynamics', Molecular Simulation, 35: 10, 812 — 821
To link to this Article: DOI: 10.1080/08927020902801555
URL: http://dx.doi.org/10.1080/08927020902801555

Molecular Simulation
Vol. 35, Nos. 10–11, September 2009, 812–821

Taylor & Francis
Taylor & Francis Group

Motions of ions in a nanoscale Paul trap from molecular dynamics

Xiongce Zhao*

Oak Ridge National Laboratory, Center for Nanophase Materials Sciences, Oak Ridge, TN 37831, USA

(*Received 10 December 2008; final version received 30 January 2009*)

Molecular dynamics simulations were used to study the motion of ions trapped inside a Paul trap of nanometre size. It is found that a single ion can be successfully trapped within nanoseconds if the applied electric voltages are in the range of hundreds of mV and the AC field has a frequency of GHz. The equilibration time and the oscillation amplitudes of the trapped ion depend on both the system temperature and applied voltages. Clusters are formed in the trap when both negatively and positively charged ions are introduced in the system, while only clusters that contain a net charge (non-neutralised clusters) can be trapped. Application of a supplemental DC driving field can effectively drive the ion off the trap centre and out of the trap. Existence of water solvent in the system helps to stabilise the trapping process.

Keywords: Paul trap; molecular dynamics; ion

PACS: 37.10.Ty; 85.35. − p; 31.15.xv

1. Introduction

The Paul trap or radiofrequency trap, which has been widely fabricated in laboratories in recent decades, is able to 'catch' and 'store' free, charged particles through ponderomotive forces generated by inhomogeneous oscillating fields [1]. It opens an effective pathway for measuring the physical properties of a single charged particle on a molecular level. Currently a large number of research groups are capable of confining ions in Paul traps and numerous investigations have been performed on the functions of the device [2]. The applications of interest span from quantum information processing [3], coherent quantum-state manipulation of trapped atomic ions [4], functional studies with fluorescent proteins [5], laser sideband cooling of the motion [6], to formation of ordered structures of trapped ions [7–11], etc.

Recently, it has been proposed that a nanometre-scale version of Paul type trap be used as a device for fast sequencing of nucleotides [12–14]. The idea is based on the concept that negatively charged DNA segments can be trapped in the device while it is driven through the trap by an electric field. Due to the strong trapping effect, each nucleotide could be maintained with specific orientations and a stable average geometry in a dynamic way. A 'nanoversion' of the Paul trap is required to reduce the conformational and orientational variations arising when the ionic bio-molecules – DNA is driving through the trap and to enhance the repeatable measurements of the base specific signature of each nucleotide. The latter was found to be critically dependent on the relative geometry of the bases to the nanopores during the DNA sequencing [15,16].

Concerns about the feasibility of a Paul trap arise as it is reduced to nanometre scale. Typical dimensions of the macroscopic Paul traps fabricated so far range from μm to cm. Great uncertainty over the effectiveness of the trap may arise when the device is scaled down to nanometre size. Possible effects could emerge from the van der Waals force from the trap walls to the particle trapped, polarisation of the medium and walls by the ion, suppression of the ion motion due to the finite size of the trap, etc. These effects can be safely neglected in a macroscopic Paul trap but may become dominant when the dimension of the trap is comparable to the molecule size, thus making the common analytic approaches ineffective in the prediction of the ion motion. Experimental studies of these concerns could be challenging and expensive. A reasonable alternative approach is molecular dynamics (MD) simulation, which can take into account the majority of the dimension and medium impacts on the feasibility of a nanoscale trap on a molecular level.

The goal of the present work is to show by MD simulations that, if fabricated, the nanoscale Paul-type trap could be an effective tool for trapping and filtering of single atomic and molecular ions. We show through a series of simulations the impact of system temperature, magnitude and frequency of applied fields, and existence of solvent, on the trapping behaviour of the device. We choose to model a conventional Paul trap model of electrodes following a hyperbolic shape to provide a proof of principle for the functionality of the nanotrap. Such a choice allows the application of analytical expressions for the resulting quadrupole electric field in the modelling,

*Email: zhaox@ornl.gov

ISSN 0892-7022 print/ISSN 1029-0435 online

DOI: 10.1080/08927020902801555
http://www.informaworld.com

which significantly simplifies the algorithms involved for numerically intensive MD simulations, without loss of generality. Analogous MD simulations can be performed for traps of other shapes using numerically calculated electric fields upon knowing the parameters of a fabricated nanotrap.

2. Theory and simulation methods

The geometry of a quadrupole trap leads to an electric potential $F(x, y, z, t)$ of approximately quadrupolar spatial shape in its centre [2]. For a charged particle, trapping is realised through a binding force that increases linearly with the distance between the particle and the trap centre. Cylindrically symmetric electrical potential is assumed in the form of

$$\Phi(r, z, t) = \frac{\Phi_0}{2r_0^2}(\alpha x^2 + \beta y^2 + \gamma z^2). \quad (1)$$

The condition that this potential has to fulfil the Laplace equation $\nabla^2\Phi = 0$ at every instant of time leads to a constraint $\alpha + \beta + \gamma = 0$ of the three geometric factors, which can be achieved in various ways, thus defining various possible geometries and types of quadrupole traps [1]. It is obvious from this constraint that the charged particle can only be trapped in a dynamical way. The frequency and voltage of the applied fields can be chosen in such a way that the time-dependent potential will give rise to a stable, approximately harmonic motion of the trapped particles, in all or chosen directions. This is in analogy to the motion of a ball rolling in a rotating saddle surface. Dynamical stability can only be achieved when the saddle is in continuous rotation.

The conventional Paul trap modelled in this study is the 3D radio frequency trap, with $\alpha = \beta = 1, \gamma = -2$ [1,2]. This trap is composed of one ring-shaped metal electrode and two cap-shaped metal electrodes, whose internal surfaces are defined as hyperbolic surfaces. A schematic of such traps is given in Figure 1. The inner surfaces of the trap coincide with equipotential surfaces.

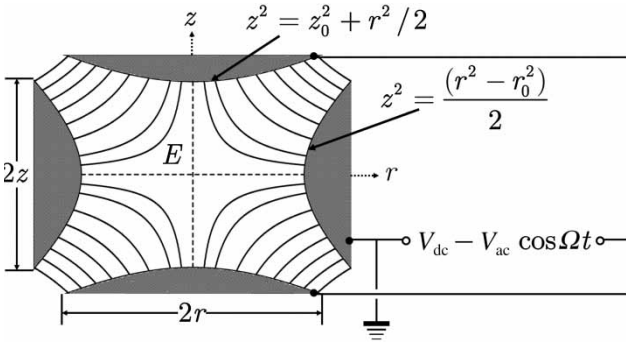

Figure 1. Schematic of a Paul trap (section of z–r plane).

The hyperbolic ring electrode is halfway between the other two electrodes, reflected by the relationship $r_0^2 = 2z_0^2$. When appropriate electric field including both AC and DC parts is applied to the system, ions can be trapped in the space between these three electrodes. For trap with dimensions from 100 μm to 1 cm, typical voltages applied are in the range of 100–300 V for V_{ac} and 0–50 V for V_{dc} with the AC frequency $f = \Omega/2\pi$ in the range of 100 kHz–100 MHz. In our simulations, the trap size is reduced to nanometre dimensions under both vacuum and aqueous filling environment.

When an electric bias of $\Phi_0 = V_{dc} - V_{ac}\cos\Omega t$ is applied to the system in Figure 1, the resulting azimuthally symmetric electric field is given by its components [1]

$$E_z = \frac{V_{dc} - V_{ac}\cos\Omega t}{z_0^2} z, \quad E_r = \frac{V_{dc} - V_{ac}\cos\Omega t}{2z_0^2} r. \quad (2)$$

The equations of motion of a particle with mass M and charge Q in this field are given by Mathieu differential equations [1],

$$\frac{d^2u}{d\tau^2} + (a - 2q\cos(2\tau))u = 0, \quad (3)$$

where u stands for either r or z coordinate, $\tau = \Omega t/2$ and

$$a = 4\frac{Q}{M}\frac{V_{dc}}{z_0^2}\frac{1}{\Omega^2}, \quad q = 2\frac{Q}{M}\frac{V_{ac}}{z_0^2}\frac{1}{\Omega^2}. \quad (4)$$

Here, $a_z = -2a_r$, $q_z = 2q_r$. The stability of the solutions to the equations, which is defined by a stable region on the a–q plane [17], is dependent on the AC and DC voltages applied, on the angular frequency Ω, on the trap dimensions, as well as on the ion charge Q and its mass M. Note that the magnitude of the voltages and the AC frequency are coupled. Therefore, the frequency of the AC voltage has to be regulated with the magnitude of the voltages in order to keep the system in the stable a–q region.

In our simulations we considered Paul-type traps (Figure 1) of two different dimensions, a small trap with $2r_0 = 5$ nm and $2z_0 = 5/\sqrt{2}$ nm, and a larger trap with $2r_0 = 50$ nm $2z_0 = 50/\sqrt{2}$ nm. The small trap is computationally less demanding in simulation but more challenging to fabricate in experiments. The larger trap is prone to be more feasible in experiments given the current etching technology, while it is more difficult to simulate due to the massive number of atoms involved. We performed most of simulations using the small trap and only performed one extensive simulation using the large trap filled with water to demonstrate the feasibility of the concept. We focus most of the analysis on the small trap because the fundamental physics for a larger trap is better understood than the nanotrap that has a dimension comparable to molecular particles.

Before each simulation, one needs to estimate the magnitude and frequency of the voltages to be applied. These can be calculated using Equation (4) by choosing appropriate values for the parameters a and q that are in the stable region [17]. Here, we used $a = 0.25$ and $q = 0.4$. Note that in certain occasions the calculated voltages using such schemes can be in the range of several volts. In applications of nanoscale Paul trap, such high voltages may cause electric breakdown to the system, depending on the trap dimensions. This additional constraint is reflected in our choice of fields. In most of our simulations the applied voltages are in the range of mV. However, this usually requires a lower AC frequency (Equation (4)) and thus a longer simulation time in order to observe a stable trapping process.

The nanoscale Paul traps used in simulations were built from a cuboid FCC gold lattice with a dimensions of $7.9 \times 7.7 \times 5.6\,\text{nm}^3$ in case of the small trap (5 nm trap hereafter) and $60 \times 60 \times 42\,\text{nm}^3$ for the large trap (50 nm trap hereafter). The internal part of the lattice was removed to create hyperbolic surfaces, consistent with the surfaces in Figure 1. A nanopore of 2 nm in diameter is created in each cap to mimic the holes that allow particles to enter the trap. One or multiple ions were placed randomly inside the trap at the beginning of each simulation, with random initial momentum conforming to a chosen system temperature. For simulations with solvent, the trap is wrapped in a box of explicit water molecules. Periodic boundary conditions are applied in all three directions.

The ions were modelled by the AMBER force field 1999 version [18]. The gold atoms composing the trap electrodes were modelled by the universal force field potentials [19]. Water molecules were modelled by the TIP3P potential [20] based on previous successful modelling of bio-molecules and ions using this model [21]. The polarisation interaction between ion/water and the gold atoms were calculated by the electrode charge dynamics (ECD) [22]. The ECD accounts for the polarisation effects of finite size metal surfaces and gives a reasonable representation of ion–metal interactions [23]. The Lennard-Jones interaction between different species were calculated by the standard Lorentz–Berthelot mixing rules with a 0.9 nm spherical cut-off without long range corrections. The particle-mesh Ewald method [24] with a fourth order interpolation and direct space summation tolerance of 10^{-5} was applied to evaluate the electrostatic interactions.

The MD simulations in vacuum were performed within the NVT (constant number of particles, constant volume and constant temperature) ensemble. For simulations including solvent, preliminary simulation under NPT (constant number of particles, constant pressure and constant temperature) ensemble with pressure of 1 bar was performed to equilibrate the solvent before NVT simulations. The temperature and pressure were kept constant wherever necessary using one of the widely employed kinetic thermostats [25]. Recently, it has been found that the newly proposed configuration thermostats [26,27] should be a more realistic choice for the non-equilibrium MD simulations of systems involving current and conductivity [28–31]. It would be interesting to probe such options for temperature control in modelling the ion-trap systems in the future.

The NAMD [32] software package was employed to integrate the equations of motion. The gold atoms were kept 'frozen' thus neglecting metal-atoms' vibrations and thermal fluctuations during the simulation. This assumes that amplitude of the vibrational oscillations of the atoms in the electrode is much smaller than the typical dimension of the trap, at the considered system temperatures (3–300 K). A typical simulation run at 300 K includes 20,000 steps of energy minimisation using a conjugate gradient algorithm, followed by gradual heating from 0 to 300 K in 3 ps, 40 ps of MD solvent equilibration, where appropriate, and 3–12 ns of production. The time step used to integrate the equations of motion was 2 fs. The electric fields used to trap the ions were turned on at the beginning of production run. In simulations with explicit solvent molecules, a 400 ps equilibration was performed after the electric fields were turned on and before the production began. The SHAKE [33] algorithm was applied to constrain the bonds involving hydrogen bonds for simulations involving water molecules. The structural configurations were collected every ps for subsequent analysis. Finally, visualisation and trajectory analysis were performed using the VMD software package [34].

3. Results and discussion

3.1 Trapping a single ion in a vacuum trap

We begin by studying the trapping of a single ion in the 5 nm trap under vacuum condition. Simulations of ions and nanotrap in vacuum are numerically less demanding than the solvated cases while providing much of the essential concept of the system. In addition, the simulation parameters preset using Equations (2)–(4) are supposed to work more reliably for a vacuum system than the solvated one due to the fact that existence of solvent molecules may confound the applicability of Equations (2)–(4). Therefore, simulation of single ion system in vacuum serves as a good test to the methodology and provides the basics for the feasibility of the concept.

One representative example result for trapping of a single chlorine ion in the 5 nm trap is given in Figure 2 at temperature of 3 K (corresponding to the ion energy of 2.5×10^{-4} eV), shown as the evolution of the ion trajectory as a function of simulation time. The initial coordinates of the ion were $(-12, 15, 24)$ Å relative to the geometric centre of the trap, which were randomly set at

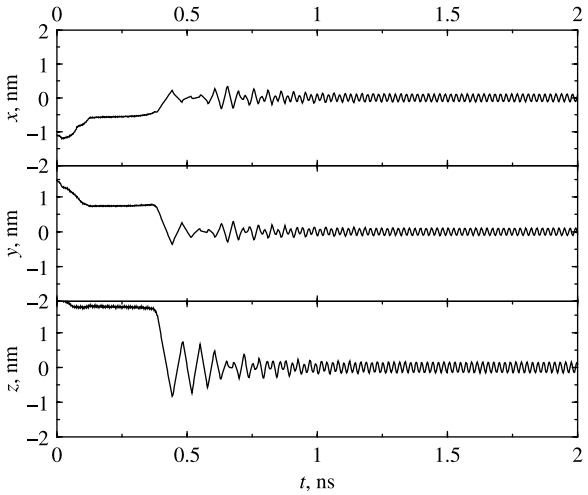

Figure 2. Simulation of a chlorine ion in the 5 nm trap at $T = 3$ K in vacuum. The trapping voltages are $V_{dc} = 200$ mV, $V_{ac} = 600$ mV with frequency of 318 GHz.

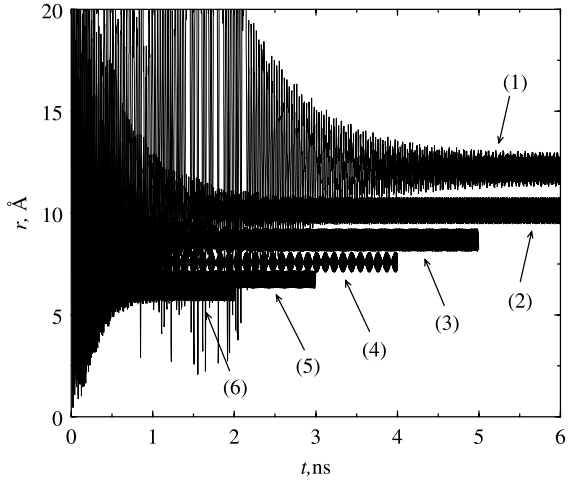

Figure 3. Dependence of stabilisation time on the magnitude of applied voltages and the frequency of AC voltages at 50 K. The simulation parameters for each line are (1) $V_{dc} = 50$ mV, $V_{ac} = 150$ mV, $f = 159$ MHz; (2) $V_{dc} = 72$ mV, $V_{ac} = 216$ mV, $f = 191$ MHz; (3) $V_{dc} = 98$ mV, $V_{ac} = 294$ mV, $f = 223$ MHz; (4) $V_{dc} = 128$ mV, $V_{ac} = 384$ mV, $f = 255$ MHz; (5) $V_{dc} = 162$ mV, $V_{ac} = 486$ mV, $f = 286$ MHz; and (6) $V_{dc} = 200$ mV, $V_{ac} = 600$ mV, $f = 318$ MHz, respectively.

the beginning of simulation. The initial momentum of the ion was randomised following a Gaussian distribution but conformed to the system temperature. The needed stable trapping voltages calculated from Equation (4) is $V_{dc} = 200$ mV and $V_{ac} = 600$ mV, with a chosen frequency of the AC voltage being 318 GHz. For a typical simulation run, the movement of the ion was monitored for 3–12 ns, depending on the time needed for a full stabilisation. Taking the results in Figure 2 as an example, it is seen that the chlorine ion is driven quickly to the centre of the trap and rotates in a circular motion. The stabilised circulating radius of the ion to the trap centre, r, is about 1.5 A. The time of about 1.0 ns is elapsed before the stabilisation is reached.

This simulation was performed for at least five times by changing the initial random number seeds that were used to generate the initial position and momenta of the ion to test the repeatability of the calculation. We found that repeated runs lead to the same quantitative conclusions as the one shown.

To study the impact of the applied trapping fields on the trapping properties, we have performed a series of simulations by varying the voltages from ($V_{dc} = 50$ mV, $V_{ac} = 150$ mV) to ($V_{dc} = 200$ mV, $V_{ac} = 600$ mV), and with frequencies ranging from 160 to 318 GHz. We notice that the AC voltage with a frequency in tens-to-hundreds of GHz range is required in order to observe a successful trapping of charged ions within a timescale of nanoseconds. In experiments, it is challenging to realise ion traps with driving fields of hundreds of GHz. But it is practically feasible to build ion traps with driving frequency of ~ 10 GHz (Reed, private communication (2007)). In our simulations, the increase in the frequency, which also implies an increase in the magnitude of the voltage according to Equation (4) for a given set of stable a and q values, results in a faster establishment of stabilisation. This is illustrated in Figure 3, which shows the simulation results using different trapping voltages and frequencies under constant temperature of 50 K. Higher trapping voltages (implying higher AC frequencies from Equation (4)) lead to a smaller circulating radius of trapped ion, and a short stabilisation time. For example, the orbiting radius of the ion decreased from about 12 to 6 Å when the AC frequency goes from 159 up to 318 GHz, accordingly the stabilisation time t_s decreased from 4.5 ns to < 1 ns. It is also found that the fluctuations in r decreases as the AC frequency f increases. In Figure 4 we present the stabilisation time and the orbiting radius of the trapped ion as a function of the AC frequency. Fitting of $t_s \sim f$ and $r \sim f$ suggests that the inverse of t_s is linearly dependent on f, while r is linearly dependent on f^{-1}, as shown by the fitted curves in the figure. Therefore, t_s goes up dramatically as f decreases (Figure 4(a)), which suggests that there exists a lower limit in the AC frequency below which one can no longer observe stable trapping for the given system. This trend is coupled with the fact that a decreasing AC frequency will result in a levelling off r around 15 Å (Figure 3).

Intuitively, the stabilisation time is dependent on the temperature, i.e. on the initial ion kinetic energy. Series of simulations at different initial temperatures were performed to study such dependence. In Figure 5 we show the stabilisation time t_s versus the temperature. The variation of the initial kinetic energy of the ion corresponds to a temperature range of 3–300 K. The simulations were performed for the 5 nm trap with the trapping voltages

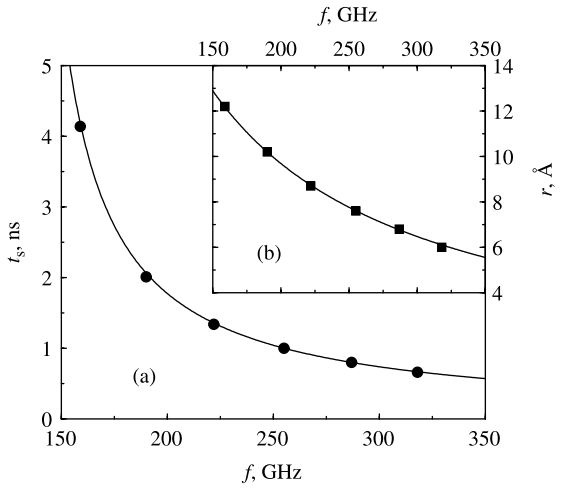

Figure 4. Dependence of stabilisation time t_s (a) and the orbiting radius r (b) of trapped ion, on the AC voltage frequency (f) at 50 K. Symbols are from individual simulations, and the lines are fitted using the relationship $t_s^{-1} = 0.0079f - 1.02$ and $r = 1933.2f^{-1} + 0.027$. Note that the magnitude of the voltage is positively correlated to the frequency in order to obtain a stabilised trapping phenomena (defined by Equation (4)).

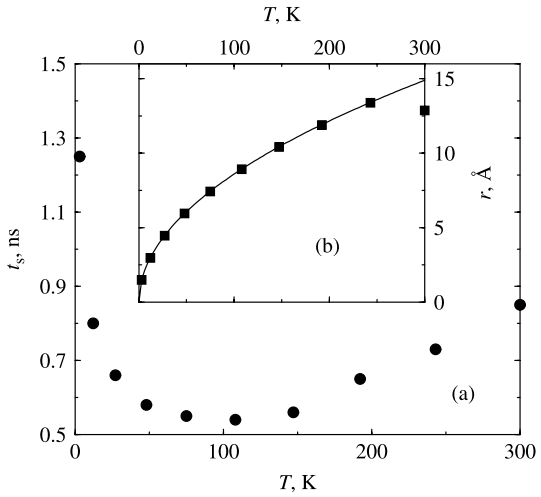

Figure 6. Temperature dependence of the stabilising time t_s (a) and orbiting radius r (b) for a chlorine ion trapped inside the 5 nm trap. The applied trapping voltages are $V_{dc} = 200$ mV, $V_{ac} = 600$ mV and $f = 318$ GHz. Symbols are from individual simulations and the curve is a fitting by $r = 0.86T^{1/2}$.

of $V_{dc} = 200$ mV, $V_{ac} = 600$ mV and $f = 318$ GHz. Interestingly, it is found that an optimal temperature that yields the fastest stabilisation exists. For a chlorine ion under the above conditions, the shortest stabilising time occurs around 50–100 K, differing by almost a factor of 2 compared with the t_s values observed at 3 and 300 K (see Figure 6(a)). As the temperature drops to near zero (below 3 K), the ion is 'frozen' at its initial position and will not be able to migrate inside the trap unless a very strong trapping field is applied. On the other hand, when the temperature is increased to above 300 K, a long time is needed for the trapping field to suppress the kinetic fluctuations of the ion.

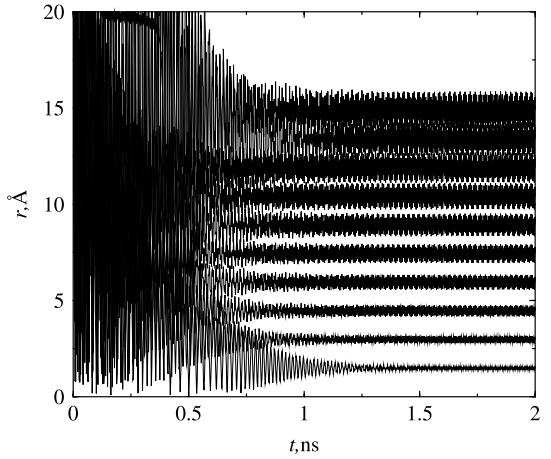

Figure 5. The stabilisation time and circulation radius of a chlorine ion inside the 5 nm trap at various temperatures. All the simulations were performed at $V_{dc} = 200$ mV, $V_{ac} = 600$ mV, and the frequency of AC voltage is 318 GHz. The simulation temperatures for each line (from top to bottom) are 300, 243, 192, 147, 108, 75, 48, 27, 12 and 3 K, respectively.

Furthermore, the circulating radius of the trapped ion inside the trap is strongly dependent on the temperature. Ion circulates with a larger radius as the temperature increases, as expected. For example, at 300 K the ion is orbiting with a radius of 15 Å whereas at 3 K the orbiting radius is only about 1.5 Å (Figure 6(b)). We also noticed that the fluctuation of r decreases as temperature drops, which is also reasonable. Careful examination of the r–T plot indicates $r^2 \propto T$. Indeed, we found that the relationship of r and T can be described excellently by a formula $r^2 = CT$, where C is a constant. The only exception is the point at $T = 300$ K (see Figure 6(b)), where r is significantly smaller than value predicted by the formula. This is simply due to the fact that the ion is confined by the 5 nm trap. That is, the ion cannot travel beyond the trap cap along the z direction. Therefore, the effective circulating orbit of the ion at 300 K is depressed. In the 300 K case, we also observed that the orbiting trajectory of trapped ion is changed slightly to adapt to the inner shape of the trap, although the circular nature of the orbit was not changed. This suggests that the motion of the ion will depend on the trap size when the trap is reduced down to nanometre scale. This phenomenon will not be present for a macroscopic Paul trap but becomes significant when the trap size is reduced to be comparable to the size of typical molecules. We deem this as one of the main limitations of a nanoscale trap in confining a charged particle. On the other hand, this effect also implies that

larger trap will tolerate an input ion with a higher energy, therefore higher temperature, without disturbing its orbiting motion in the z direction.

3.2 Application of additional driving field

In practical application of the nanotrap proposed in this study, an extra driving field can be applied along the z-axis (Figure 1) to guide the ion into the trap. For this reason, we performed simulations to study the system under such an additional influence. We again used the chlorine ion in the 5 nm trap as an example, with additional DC field ranging from 10 to 150 mV/nm applied along the z direction. Initially the ion was placed at the entrance of one of the cap holes in the trap with its coordinate as $(-7, 5, 22)$ Å relative to the trap centre, with the initial momentum of the ion conforming to the system temperature. The z-direction driving field and the trapping fields were turned on simultaneously when the simulation starts, and the trajectory of the ion was monitored. One result from such simulations is presented in Figure 7. Here, we used a temperature of 3K to suppress the fluctuations in the coordinates, due to the reason stated in previous sections, to obtain a clear picture on how the ion will react to the additional z-field in each direction. It is seen that the ion migrates rapidly through the central region from one entrance along the z-direction, while orbiting around the trap centre in the x–y plane. For the results shown in Figure 7, the additional DC field along the z-axis was 25 mV/nm. Under the z-field of this magnitude, the ion was finally stabilised at a position of about $(0, 0, -8)$ Å. The corresponding orbiting radius of the ion was about 0.8 nm. That is, the ion is trapped similarly like being trapped without the z-direction DC field but its position is now significantly shifted along the z axis.

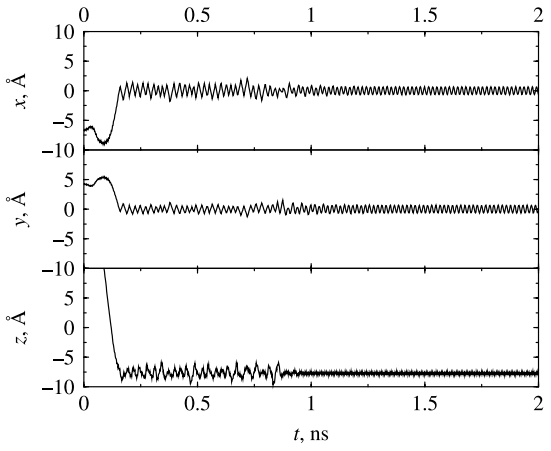

Figure 7. Trapping of a chlorine ion inside the 5 nm trap with a biased voltage along the axis through the two holes in the caps. The simulation was performed at 3 K, with $V_{dc} = 200$ mV, $V_{ac} = 600$ mV and $f = 318$ GHz. The driving field along the z axis is 25 mV/nm.

We have carried out series of simulations using z-fields of various strengths and found that the expected shift of the ion orbit along the z-axis increases with the increase of strength of the z-field. However, the ion was driven all the way through the trap as soon as a threshold z-field is reached. For the 5 nm trap with trapping voltages of $V_{dc} = 200$ mV, $V_{ac} = 600$ mV and $f = 318$ GHz, we found that the ion is stably trapped when the z field is below 110 mV/nm, while a field of 125 mV/nm would drive the ion through the trap in <1 ns, without ever reaching a stabilised trapping. This suggests that for the 5 nm trap under the current trapping conditions, the threshold z-field for driving the ion through the whole trap lies in 110–125 mV/nm. It is expected from this observation that it is possible to drive the ion back and forth along the z-axis through the trap, if an alternating field is applied in the z-axis, similar to that found in a previous study of DNA translocation in nanopores [35].

3.3 Trapping multiple ions

With the knowledge from simulations of trapping a single ion, next we are interested in investigating the trapping of multiple ions in a nanotrap under vacuum condition. We start our simulation by placing five pairs of chlorine and sodium ions in the 5 nm trap, with the initial coordinates of each pair of Cl^-/Na^+ set randomly inside the trap. We note that by 'pair' here we refer to the fact that each chlorine ion placed in the trap is associated by a sodium ion, with their centre of mass distance being about 3–5 Å. This is a natural set-up commonly used by many standard MD simulation packages such as AMBER [36]. We also performed simulations with chlorine and sodium ions placed randomly at the beginning of the simulation and found that they will form pairs within hundreds of simulation time steps because of the strong long range electrostatic interaction between any particles with opposite charges.

We found that scattered ion pairs will form ion clusters as the simulation proceeds. The number of cluster decreases rapidly as a function of simulation time. Therefore, it is necessary and convenient to monitor the motion of the clusters as well as the trajectory of each individual ion. Here, we employed the technique developed by Sevick et al. [37] to obtain the cluster statistics during the simulation. A cluster is defined as any particles that form a 3D aggregate with the pairwise distance between any two ions being <5 Å, which is about the Lennard-Jones distance between a Cl^-/Na^+ pair. A connectivity matrix can be calculated at every MD time step and the number of clusters (which equals to the rank of the connectivity matrix) in the system can be recorded as a function of simulation time. A detailed description of the algorithm can be found in the original literature [37].

In Figure 8 we present the simulation results for five pairs of chlorine and sodium ions in the 5 nm trap.

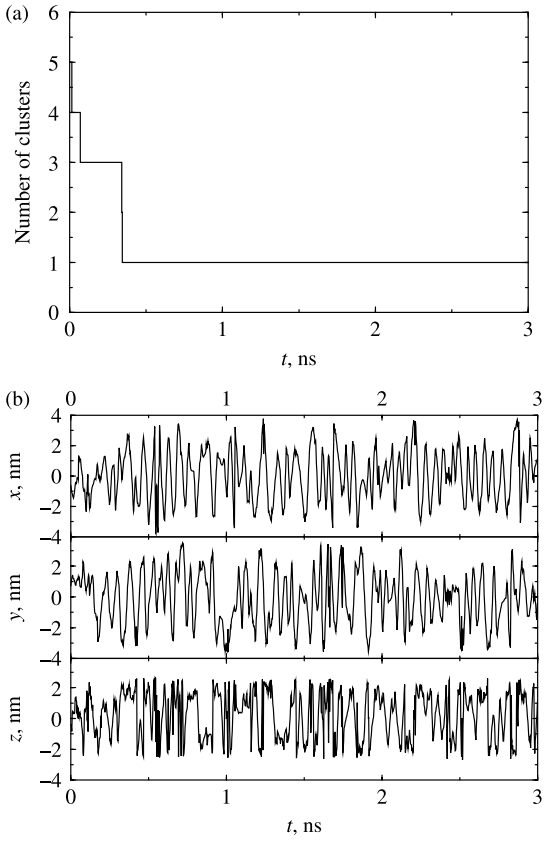

Figure 8. Trapping of five pairs of Cl^-/Na^+ ions inside a vacuum trap at 300 K. The trapping voltages are $V_{dc} = 200$ mV, $V_{ac} = 600$ V and $f = 318$ GHz. (a) The evolution of number of clusters in the system and (b) the coordinates of the centre of mass of ions as a function of time.

The evolution of the number of clusters in the system is depicted in Figure 8(a), and the trajectory of the centre of mass of all 10 ions is shown in Figure 8(b). It can be seen that the initial number of clusters is 5, which indicates that the five ion pairs are scattered in the trap. As the simulation proceeds, the ion pairs quickly aggregate with each other to form bigger clusters. Correspondingly the number of clusters drops. By $t = 0.4$ ns, a single cluster was formed and stabilised. The stepwise nature of the line in Figure 8(a) indicates that the formed single cluster is energetically very favourable compared with scattered clusters.

However, we found that the ion cluster formed by the five chlorine and five sodium ions was never trapped stably in the nanotrap. This is clearly seen from the trajectory shown in Figure 8(b). The random fluctuation of the coordinates along each direction indicates that the movement of the ion clusters is Brownian in nature instead of a stable orbiting behaviour like those observed previously for a stably trapped particle. Actually the ion cluster was moving everywhere in space given the fact that the system was periodic in all three directions. This is not surprising considering the neutral nature of the cluster formed by even number of chlorine and sodium ions. It is noticed that the geometric shape of the cluster is changing dynamically during the simulation, although the cluster is quite intact by itself. Such a shape deformation will obviously result in instantaneous polarity in the cluster. But it is also clear that such polarity is not sufficient to make the cluster being trapped under the current simulation conditions.

With this in mind, naturally our next target is to simulate the trapping of uneven number of chlorine and sodium ions in the trap. Different from the last simulation, this time three chlorine ions and two sodium ions were introduced, to make the system non-neutral. As expected, such a setup results in a successful trapping. As seen in Figure 9, initially we have three clusters in the system, two Cl^-/Na^+ pairs and one single chlorine ion. Very quickly the ions form a single cluster, as shown in Figure 9(a). But different from the previous simulation, the ion cluster was trapped at the centre of the nanotrap in less than 0.3 ns once the final single cluster is formed, apparently due to the

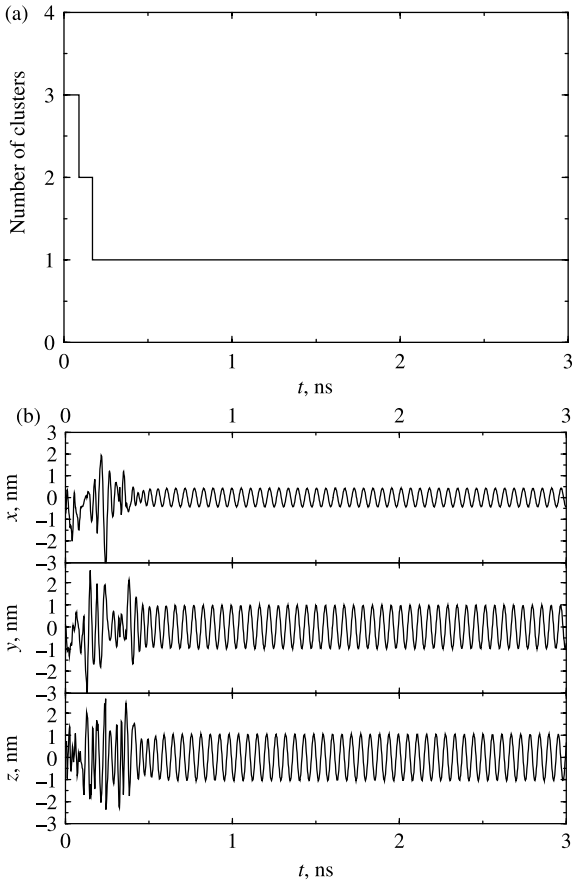

Figure 9. Trapping of three Cl^- and two Na^+ ions inside a vacuum trap at 300 K. The trapping voltages are $V_{dc} = 200$ mV, $V_{ac} = 600$ V and $f = 318$ GHz. (a) The evolution of number of clusters in the system and (b) the coordinates of the centre of mass of ions as a function of time.

net negative charge in the cluster. This observation is depicted by the trajectory in Figure 9(b). Like before, the trapped ion cluster circulates around the trap centre, with the circulating radius being about 10.5 Å.

3.4 Trapping an ion in a solvated trap

Simulation results obtained so far suggest that a nanoscale Paul trap is capable of trapping ions at least under vacuum condition. It is also evident that the Mathieu equation (Equation (3)) is valid in predicting the stable trapping parameters of the system under vacuum condition. However, these predictions are not as certain in the presence of explicit solvent background, due to the damping force from the viscosity of the solvent molecules [38,39]. If the viscosity force can be modelled by $F = -Dv$, where v is the instantaneous velocity of the ion in the trap, and D is an unknown constant dependent on the viscosity constant and ion-water interaction, the Mathieu equation will be modified as

$$\frac{\mathrm{d}^2 w}{\mathrm{d}\tau} + \left[a - \left(\frac{D}{M\Omega}\right)^2 q\cos(2\tau)\right] w = 0, \qquad (5)$$

where $w = ue^{k\tau}$. The damping force will shift and change the size of the stable region on the a–q plane. The collisions between the solvent and the ion will influence the trajectory of the ion by increasing or decreasing its energy depending on the relative mass of the ion and solvent molecule. In our study, the ion of interest, chlorine, is about twice heavier than the water molecule. Therefore, we expect a stabilising effect on the oscillation movement of the ion from the background solvent.

There are at least two different approaches to include the solvent effect in the modelling of an aqueous environment. We can either use implicit solvent models or use explicit water molecules. The implicit models could be a useful choice for analysis of macroscopic traps filled with water, but is not suitable for modelling a trap of nanometre size due to the significant dielectric inhomogeneities through the nano trap volume. In our study, we model the solvent as explicit water molecules.

As testing cases, we performed several trial simulations using the 5 nm trap filled with water. All the simulations were performed at 300 K since the water potential employed can only give reasonable results at this temperature range. The trapping voltages are estimated from Equation (4) re-scaled to the dielectric constant of water. This allows us to use a higher voltage and lower frequency compared with the vacuum cases. For example, we tried simulations using $V_{dc} = 4$ V, $V_{ac} = 8$ V, $f = 80$ GHz. We observed stable trapping phenomena for most of these trials, which were reported in a previous work [14], although usually a longer simulation time is needed to reach full stabilisation. On the other hand, it is found that the ion experiences much less fluctuations in the movement during the stabilising process along any of the directions, with the much smaller final oscillation amplitude of the ion in comparison with that for the same ion trapped in a vacuum trap under the same temperature.

We also observe that the presence of explicit solvent helps to stabilise the trapping process. We have performed a series of simulations using various combinations of trapping voltages and frequencies, such as $V_{dc} = 2$ V, $V_{ac} = 6$ V, $f = 20$ GHz; $V_{dc} = 1$ V, $V_{ac} = 3$ V, $f = 20$ GHz. Some of these parameters do not satisfy strictly the stable region defined by Equation (4) (with or without correction to the water dielectric constant). Interestingly, in all these cases we could observe stable trapping. It is evident that the range of stabilisation defined by parameters a and q is significantly enlarged in the presence of the damping with water, as discussed above. It would be useful to estimate the new stable region on the a–q plane using the modified Equation (5). However, constants such as D need to be fitted, either by analytical approach or systematic simulations.

Finally, we consider an example with the solvated 50 nm trap, aiming to model a system that is realistic to experimental devices proposed. This simulation is numerically much more extensive than the ones with the 5 nm trap, due to a significant number of explicit water molecules included. However, the increased dimensions of the trap allow for lower (and more realistic) trapping AC field frequencies, here chosen to be 20 GHz, and larger electric biases before a possible breakdown occurs. One chlorine ion was initially positioned at (110, 100, 88) Å inside the trap and the initial kinetic energy of the ion and water conforms to a system temperature of 300 K. The trapping voltages were $V_{dc} = 200$ mV, $V_{ac} = 600$ mV with frequency of 20 GHz, which were turned on at $t = 0$.

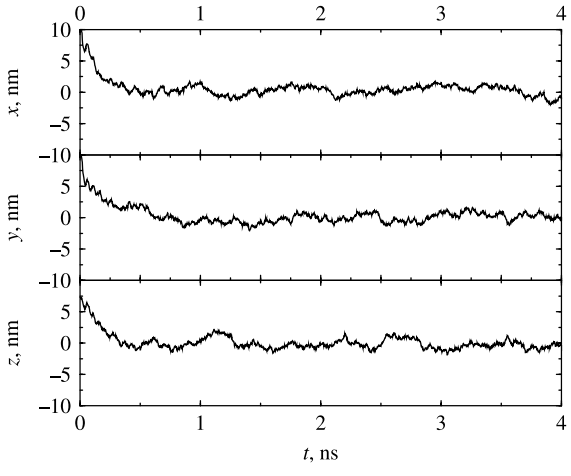

Figure 10. Trapping of a chlorine ion inside the 50 nm Paul trap filled with water at 300 K. The trapping voltages are $V_{dc} = 200$ mV, $V_{ac} = 600$ mV and $f = 20$ GHz.

We note that the trapping fields in this run were not estimated from Equation (4) but based on empirical values from the 5 nm solvated trap simulations. The results from this simulation are given in Figure 10. It can be seen that the ion was trapped at the centre of the trap after about 1 ns, with the orbital radius of about 14 Å. Again, the fluctuations in the coordinates of ion in each direction are much smaller compared with those observed in vacuum condition. However, the oscillation of ion around the trap centre lacks the periodicity of that for an ion in vacuum, possibly due to the thermo effects in the solvent.

4. Conclusions

We carried out extensive MD simulation to study the properties of a nanoscale Paul trap in trapping single or multiple ions. We found that trapping of low-energy charged ions in Paul traps of nanometre size is feasible both under vacuum and solvated conditions. The typical trapping time is in a timescale of nanoseconds if an AC field of tens to hundreds of GHz is applied. The trapped ion circulates around the centre of the vacuum trap, with the circulating radius depending on the trapping fields applied and system temperature. Higher AC frequencies result in a smaller circular radius and a faster stabilisation time. On the other hand, there appears to exist an optimal temperature for a fast-trapping process.

The position of an trapped ion inside the nanotrap can be easily controlled by applying extra DC fields to the system. This was demonstrated by applying an additional driving field along the z-direction of the trap. The trapped ion is effectively shifted to one side along the z-axis if the extra field is not strong enough to drive the ion all the way through the trap. Multiple ions with opposite charges can form stable clusters inside the trap. But only ion cluster with non-neutralised net charges can be successfully trapped. Our simulations also indicate that ions can be trapped in a solvated nanotrap. The damping force from the solvent helps to stabilise the trapping process and effectively increases the choices in the trapping fields for a stable trapping. In addition, the movements of ions in a solvated trap experience less fluctuations compared with those observed in a vacuum trap, although the stabilisation time in a solvated trap is usually longer.

Acknowledgements

The author is grateful to Predrag S. Krstic and Peter T. Cummings for insightful discussions. This research was supported by the Center for Nanophase Materials Sciences, which is sponsored at Oak Ridge National Laboratory by the Division of Scientific User Facilities of US DOE, at ORNL managed by a UT-Battelle for the US DOE under Contract No. DEAC05-00OR22725. This research used resources of the National Energy Research Scientific Computing Center, which is supported by the Office of Science of the US DOE under Contract No. DE-AC02-05CH11231.

References

[1] W. Paul, *Electromagnetic traps for charged and neutral particles*, Rev. Mod. Phys. 62 (1990), pp. 531–540.
[2] D. Leibfried, R. Blatt, C. Monroe, and D. Wineland, *Quantum dynamics of single trapped ions*, Rev. Mod. Phys. 75 (2003), pp. 281–324.
[3] S. Seidelin, J. Chiaverini, R. Reichle, J.J. Bollinger, D. Leibfried, J. Britton, J.H. Wesenberg, R.B. Blakestad, R.J. Epstein, D.B. Hume et al., *Microfabricated surface-electrode ion trap for scalable quantum information processing*, Phys. Rev. Lett. 96 (2006), 253003.
[4] D.J. Wineland, C. Monroe, W.M. Itano, D. Leibfried, B.E. King, and D.M. Meekhof, *Experimental issues in coherent quantumstate manipulation of trapped atomic ions*, J. Res. NIST 103 (1998), pp. 259–328.
[5] U. Rothbauer, K. Zolghadr, S. Muyldermans, A. Schepers, M.C. Cardoso, and H. Leonhardt, *A versatile nanotrap for biochemical and functional studies with fluorescent fusion proteins*, Mol. Cell. Proteomics 7 (2008), pp. 282–289.
[6] K. Abich, A. Keil, D. Reiss, C. Wunderlich, W. Neuhauser, and P.E. Toschek, *Thermally activated hopping of two ions trapped in a bistable potential well*, J. Opt. B 6 (2004), pp. S18–S23.
[7] J.P. Schiffer, *Order in confined ions*, J. Phys. 36 (2003), pp. 511–523.
[8] L. Shi, X.W. Zhu, M. Feng, and X.M. Fang, *Ordered structures of a few ions in the Paul trap*, Commun. Theor. Phys. 31 (1999), pp. 491–496.
[9] W.M. Itano, J.C. Bergquist, J.J. Bollinger, and D.J. Wineland, *Cooling methods in ion traps*, Phys. Scr. T59 (1995), pp. 106–120.
[10] H. Walther, *From a single-ion to a mesoscopic system--crystallization of ions in Paul traps*, Phys. Scr. T59 (1995), pp. 360–368.
[11] C.S. Edwards, P. Gill, H.A. Klein, A.P. Levick, and W.R.C. Rowley, *Laser-cooling effects in few-ion clouds of YB+* , Appl. Phys. B 59 (1994), pp. 179–185.
[12] D. Arnott, W.J. Henzel, and J.T. Stults, *Rapid identification of comigrating gel-isolated proteins by ion trap mass spectrometry*, Electrophoresis 19 (1998), pp. 968–980.
[13] H. Oberacher, W. Parson, P.J. Oefner, B.M. Mayr, and C.G. Huber, *Applicability of tandem mass spectrometry to the automated comparative sequencing of long-chain oligonucleotides*, J. Am. Soc. Mass Spectrom. 15 (2004), pp. 510–522.
[14] X.C. Zhao and P.S. Krstic, *A molecular dynamics simulation study on trapping ions in a nanoscale Paul trap*, Nanotechnology 19 (2008), 195702.
[15] J. Lagerqvist, M. Zwolak, and M. Di Ventra, *Influence of the environment and probes on rapid DNA sequencing via transverse electronic transport*, Biophys. J. 93 (2007), pp. 2384–2390.
[16] V. Tabard-Cossa, D. Trivedi, M. Wiggin, N.N. Jetha, and A. Marziali, *Noise analysis and reduction in solid-state nanopores*, Nanotechnology 18 (2007), 305505.
[17] H. Winter and H.W. Ortjohann, *Simple demonstration of storing macroscopic-particles in a Paul trap*, Am. J. Phys. 59 (1991), pp. 807–813.
[18] D.A. Case, T.E. Cheatham, T. Darden, H. Gohlke, R. Luo, K.M. Merz, A. Onufriev, C. Simmerling, B. Wang, and R.J. Woods, *The Amber biomolecular simulation programs*, J. Comput. Chem. 26 (2005), pp. 1668–1688.
[19] A.K. Rappe, C.J. Casewit, K.S. Colwell, W.A. Goddard, and W.M. Skiff, *UFF, a full periodic-table force-field for molecular mechanics and molecular dynamics simulations*, J. Am. Chem. Soc. 114 (1992), pp. 10024–10035.
[20] W.L. Jorgensen, J. Chandrasekhar, J.D. Madura, R.W. Impey, and M.L. Klein, *Comparison of simple potential functions for simulating liquid water*, J. Chem. Phys. 79 (1983), pp. 926–935.
[21] T.E. Cheatham and M.A. Young, *Molecular dynamics simulation of nucleic acids: successes, limitations, and promise*, Biopolymers 56 (2000), pp. 232–256.
[22] C.G. Guymon, R.L. Rowley, J.N. Harb, and D.R. Wheeler, *Simulating an electrochemical interface using charge dynamics*, Condens. Matter Phys. 8 (2005), pp. 335–356.

[23] C.M. Payne, X.C. Zhao, L. Vlcek, and P.T. Cummings, *Molecular dynamics simulation of ss-DNA tranlocation through a copper nanoelectrode gap*, J. Phys. Chem. B 112 (2008), pp. 1712–1717.
[24] T. Darden, D. York, and L. Pedersen, *Particle mesh Ewald-an Nlog(N) method for Ewald sums in large systems*, J. Chem. Phys. 98 (1993), pp. 10089–10092.
[25] H.J.C. Berendsen, J.P.M. Postma, W.F. Vangunsteren, A. Dinola, and J.R. Haak, *Molecular dynamics with coupling to an external bath*, J. Chem. Phys. 81 (1984), pp. 3684–3690.
[26] B.D. Butler, G. Ayton, O.G. Jepps, and D.J. Evans, *Configurational temperature: verification of Monte Carlo simulations*, J. Chem. Phys. 109 (1998), pp. 6519–6522.
[27] K.P. Travis and C. Braga, *Configurational temperature control for atomic and molecular systems*, J. Chem. Phys. 128 (2008), 014111.
[28] J. Petravica and J. Delhommelle, *Conductivity of molten sodium chloride and its supercritical vapor in strong dc electric fields*, J. Chem. Phys. 118 (2003), pp. 7477–7785.
[29] J. Petravica and J. Delhommelle, *Conductivity of molten sodium chloride in an alternating electric field*, J. Chem. Phys. 119 (2003), pp. 8511–8518.
[30] J. Delhommelle, *Should "lane formation" occur systematically in driven liquids and colloids?*, Phys. Rev. E 71 (2005), 016705.
[31] C. Desgranges and J. Delhommelle, *Molecular simulation of transport in nanopores: application of the transient-time correlation function formalism*, Phys. Rev. E 77 (2008), 027701.
[32] J.C. Phillips, R. Braun, W. Wang, J. Gumbart, E. Tajkhorshid, E. Villa, C. Chipot, R.D. Skeel, L. Kale, and K. Schulten, *Scalable molecular dynamics with NAMD*, J. Comput. Chem. 26 (2005), pp. 1781–1802.
[33] J.P. Ryckaert, G. Ciccotti, and H.J.C. Berendsen, *Numericalintegration of cartesian equations of motion of a system with constraints-molecular dynamics of n-alkanes*, J. Comput. Phys. 23 (1977), pp. 327–341.
[34] W. Humphrey, A. Dalke, and K. Schulten, *VMD: Visual molecular dynamics*, J. Mol. Graph. 14 (1996), pp. 33–38.
[35] X.C. Zhao, C.M. Payne, and P.T. Cummings, *Controlled translocation of DNA segments through nanoelectrode gaps from molecular dynamics*, J. Phys. Chem. C 112 (2008), pp. 8–12.
[36] D.A. Case, T.A. Darden, T.E. Cheatham, III, C.L. Simmering, J. Wang, R.E. Duke, R. Luo, K.M. Merz, B. Wang, D.A. Pearlman, et al., *Amber 8.0*, University of California, San Francisco, 2004.
[37] E.M. Sevick, P.A. Monson, and J.M. Ottino, *Monte Carlo calculations of cluster statistics in continuum models of composite morphology*, J. Chem. Phys. 88 (1988), pp. 1198–1206.
[38] M. Nasse and C. Foot, *Influence of background pressure on the stability region of a Paul trap*, Eur. J. Phys. 22 (2001), pp. 563–573.
[39] T. Hasegawa and K. Uekara, *Dynamics of a single-particle in a Paul trap in the presence of the damping force*, Appl. Phys. B 61 (1995), pp. 159–163.